



DALGONA

RF based Antenna Tracking System

Version 1.0

Date: 25.05.2025

Design Studio Section: 4

Presented by:

Alkım Bozkurt

Emirhan Yolcu

Sevda Sıla Yıldız

Özgür Akyaz

Bora Özkan

Table of Contents

Table of Contents	2
Executive Summary	3
Introduction.....	4
Background and Motivation	4
Problem statement.....	4
Scope and organization of the report	5
Requirement Analysis.....	5
Overall System Description.....	7
Top level architecture and Block Diagram	7
Technical Drawing and 3D Model	9
Subsystem Compatibility and Integration	11
Interface Analysis	11
Hardware and Software Synchronization	13
Subsystem Overviews.....	13
Compatibility with Requirements	20
Discussion of Engineering Trade-offs	21
Test Procedure	21
Test Setup.....	22
Results and Evaluation	23
Resource Management	25
Cost Analysis.....	25
Power Analysis	27
Schedule Analysis	29
Discussions.....	30
Conclusion.....	31
References	32
Appendix.....	33
User Manual	37
1. INTRODUCTION.....	40
2. SYSTEM OVERVIEW	40
3. SAFETY GUIDELINES	41
4. HARDWARE COMPONENTS.....	41
5. SOFTWARE INTERFACE (GUI)	42

6. FEATURE GUIDE	42
7. SYSTEM SETUP	43
8. OPERATING INSTRUCTIONS	44
10. TROUBLESHOOTING	44
11. MAINTENANCE AND BATTERY HANDLING	44
13. ENVIRONMENTAL AND SAFETY COMPLIANCE	45
14. REGULATORY NOTES	45
15. CONTACT AND SUPPORT	45

Executive Summary

This report presents the Final Report of the RF-based Antenna Tracking System (RFATS), a real-time tracking platform developed to maintain reliable wireless communication with mobile transmitters in GPS-denied or jamming-prone environments. Designed with adaptability, compactness, and responsiveness in mind, the system leverages directional RF sensing and mechanical alignment to preserve continuous signal lock between a receiver and a mobile RF source.

The system operates by estimating the direction of arrival of RF signals through phase difference analysis between two spatially separated directional receiver antennas. This estimation is translated into steering commands that adjust the antenna's orientation in both azimuth and elevation, enabling continuous tracking within an angular error margin of 5 degrees. The signal processing and control logic are implemented in C++, running on a Raspberry Pi platform.

Core architectural components such as the antenna configuration, direction estimation strategy, and two-axis mechanical tracking structure have been finalized. Early-stage tests confirmed the validity of the direction estimation method at short to medium ranges and demonstrated mechanical responsiveness within required angular speeds and positioning tolerances. However, practical tests revealed increasing angle error in large-range movements, primarily due to servo motor limitations. To address this, a transition to stepper motors is under consideration for azimuth control. While this change is expected to improve tracking continuity, it introduces risks in mechanical integration and control stability that are acknowledged and evaluated in the relevant sections of this report.

The direction estimation module has also shown degradation in accuracy at longer distances, likely due to environmental interference and limitations in antenna separation. Planned mitigation strategies include refined antenna layout and noise-aware signal processing adjustments. Integration between the estimation output and mechanical actuation is ongoing, and full closed-loop operation is targeted for the next design phase.

In summary, RFATS has reached a mature design state, with validated subsystems and well-defined performance targets. Major system components are in place, and ongoing development focuses on mechanical optimization and full subsystem integration. Remaining technical risks are identified and addressed throughout this report. Upon completion, the system is expected to offer a flexible, interference-resilient tracking capability suitable for use in UAV communication, disaster response, and military scenarios.

Introduction

Background and Motivation

In modern communication systems, maintaining a stable wireless connection with mobile units is critical across a wide range of applications, from military operations to disaster response and UAV navigation. Traditional tracking systems often rely on GPS or explicit location data to maintain alignment between the transmitter and receiver. However, such dependencies become unreliable or entirely infeasible in GPS-denied environments or under intentional signal jamming. In these cases, communication stability becomes vulnerable, risking signal loss and degraded performance.

The RF-based Antenna Tracking System (RFATS) addresses these challenges by eliminating the need for location data, instead using RF signal sensing to estimate and track the direction of the transmitting unit. By calculating the steering angle based on signal characteristics such as phase differences, the system can dynamically adjust its antenna orientation to maintain lock on the source, even when the environment is noisy or unpredictable. This capability is especially relevant in remote operations where infrastructure may be unavailable.

From a technical perspective, the motivation behind RFATS is to combine robustness, modularity, and real-time responsiveness into a lightweight and cost-effective solution. Using software-defined radio (SDR) hardware and embedded processing, the system aims to meet strict angular accuracy and reaction time constraints, all while resisting interference and reducing reliance on fragile infrastructure. This approach reflects a growing demand in modern communication systems for adaptable and self-sufficient tracking mechanisms that can perform reliably under real-world constraints.

Problem statement

The core engineering problem addressed by this project is the real-time tracking of a mobile RF transmitter using only signal reception data, without any external positioning input. Specifically, the task is to rotate a directional receiver system to maintain optimal alignment with a moving source that emits RF signals, even in the presence of interference and environmental noise.

To meet its objectives, the system must dynamically rotate its receiver antenna to maintain accurate alignment with the moving RF source. This involves estimating the transmitter's direction through signal processing — primarily phase difference analysis across two spatially separated directional receiver antennas — and translating this estimation into motor control commands for azimuth and elevation adjustment.

Key performance targets include an angular error of less than 5 degrees RMS, a tracking lock time under 3 seconds, and a minimum tracking speed of 15 degrees per second in the azimuth axis. The system must also remain functional in jamming environments with defined interference characteristics.

The problem requires developing a compact, modular, and cost-effective system that integrates signal estimation algorithms, directional RF front-end design, and mechanical actuation. It must perform reliably in changing and potentially hostile environments, without manual recalibration or dependency on fragile infrastructure. RFATS must autonomously adapt to the transmitter's motion and signal behavior in real-time, ensuring stable and responsive operation under diverse conditions.

Scope and organization of the report

This report documents the current design status, validation efforts, and development plan of the project. It outlines the system architecture and its subsystems as they stand at the critical design stage, where most major design decisions have been implemented or are in the final stages of refinement. The report captures not only the finalized elements but also identifies areas where continued development, integration, or adjustment is anticipated. These points are discussed transparently, along with the risks they may introduce.

The report begins with a description of the overall system, including its block architecture, subsystem roles, and physical modeling efforts. Following this, the requirement analysis section traces customer needs to measurable performance objectives and system constraints. Subsystem compatibility and integration topics are then explored, including the communication and synchronization mechanisms that support cross-functional operation.

Design modifications since the Critical Design Review Report are highlighted in a dedicated section, including justifications for changes and evaluation of trade-offs. The test procedure and evaluation results section reflect performance metrics obtained from individual and partial system tests. Resource management is addressed in terms of cost, power, and project scheduling. The report concludes with a summary of progress and outlines the key development steps leading to the final implementation.

Throughout the project, responsibilities were divided across team members based on technical background. Team members contributed to signal processing, RF front-end design, motor control systems, embedded software development, mechanical design, and system testing. The modular structure of RFATS allowed parallel development of subsystems, followed by coordinated integration phases. This report reflects the collective outcomes of those efforts.

Requirement Analysis

The RF-based Antenna Tracking System (RFATS) is developed to ensure robust, GPS-independent signal tracking by estimating the direction of arrival (DoA) of RF signals and aligning a directional receiver antenna accordingly. System and subsystem level requirements have been finalized and structurally defined based on the mission objectives and performance expectations established in the conceptual design phase. These requirements address functional, mechanical, electronic, and software components in a cohesive and interdependent framework, ensuring that the design meets all operational constraints under realistic use conditions.

At the system level, the platform must maintain a reliable line-of-sight (LOS) communication link with a moving RF source. To accomplish this, the tracking mechanism must rotate the receiving antenna in azimuth and elevation axes with a root-mean-square angular error below 5 degrees. The system must acquire and lock onto a new target within 3 seconds and maintain angular tracking speeds of at least 15 degrees per second in azimuth. These performance metrics are derived from use-case scenarios involving mobile transmitters such as UAVs, where high responsiveness and minimal latency are critical for maintaining data flow and signal integrity.

To fulfill these specifications, each subsystem has been developed around its respective requirements. The receiving antenna module features a hybrid arrangement of Yagi-Uda and Vivaldi antennas, combined via a real-time controlled RF switch to enable dual-axis spatial

sampling using a reduced number of coherent SDR channels. Requirements for this module include sufficient antenna gain and directivity to operate reliably in the 2 GHz band, physical alignment within spatial tolerances to preserve phase coherence, and compatibility with the signal processing chain. Signal sampling is managed by an ADALM-PLUTO SDR, which is required to deliver accurate, time-aligned I/Q data with minimal phase distortion across switching cycles.

The processing module, centered around the Raspberry Pi 5, is responsible for executing high-resolution DoA estimation using Root-MUSIC and correlation-based alignment algorithms. Requirements for this module include the ability to interface with both the SDR and motor control systems via serial and USB protocols, ensure sub-second latency from signal capture to motor actuation command, and maintain computational integrity while running a C++ implementation of the processing pipeline. The software must also sustain processing performance in the presence of environmental noise and jamming, including real-time detection of signal degradation and fallback behavior when signal is lost.

Mechanical requirements emerged from the need for precise and stable antenna orientation. On the azimuth axis, the NEMA 23 stepper motor—controlled via a TB6600 driver—is required to deliver 360° continuous rotation with microstepping capability and maintain stability under payload torque. On the elevation axis, testing showed that the required holding torque exceeded 50 kg·cm. As a result, the finalized requirement for this axis is a motor with sufficient stall torque and braking performance to support bi-directional movement under gravitational loading. The entire motor subsystem must maintain responsiveness within the required angular speed and positioning tolerances, while avoiding overshoot and mechanical oscillation.

The control subsystem—implemented on an Arduino Uno—must interpret directional commands from the Raspberry Pi and generate precise PWM, direction, and enable signals for the motors. The controller must account for variable torque conditions, implement acceleration/deceleration profiles, and allow dynamic speed control without feedback oscillation. Communication between Pi and Arduino must be stable under load and capable of real-time command execution.

Power and thermal requirements dictate that all components must be supported by a 3-cell Li-Po battery of 2800 mAh, capable of simultaneously powering the Raspberry Pi, motor drivers, and RF frontend. This module must include voltage monitoring and over-discharge protection, with wiring designed for high current tolerance and thermal resilience. Total power consumption is expected to remain under 15 W during normal operation, allowing extended runtime within portable deployment conditions.

Finally, the overall system must maintain mechanical compactness and modularity. Physical integration of components must allow for maintenance, cable routing, and protection against mechanical shock and RF interference.

Taken together, these finalized requirements form a complete, relevant, and inclusive specification set that maps directly to the functional and environmental challenges of the RFATS system. Each subsystem requirement has been derived and validated through analytical modeling, simulation, and real-world testing, ensuring traceability to the project objectives and compatibility across all interfaces.

Overall System Description

Our project aims to develop an RF-based antenna tracking system designed to autonomously follow the direction of a UAV or RF-emitting target object in motion, using real-time received signals and implementing high-level signal processing techniques on them. The system's core objective is to maximize communication link quality by keeping a LOS (Line of sight) between the target and the receiving unit.

Most similar products in the market employ omnidirectional antennas to keep a LOS between a moving target and a stationary receiving station. Our product is designed in a way so that we can use directional antennas and maintain a communication link. The main advantage of our product is as we are using a directional antenna, we can provide a higher SNR, a better communication quality and a lower power consumption.

The highlight of our system is it utilizes the RF signals emitted from the target and eliminates the use of GNSS signals. This is particularly useful in scenarios where the tracked object (e.g., a UAV) is equipped with a radio transmitter and where traditional GPS-based tracking is not viable or sufficiently precise.

Top level architecture and Block Diagram

The product is designed in detail and with extensive engineering solutions to overcome challenges. Our system consists of several sub-blocks, each having a crucial role in the overall architecture. Figure 1 describes the overall system architecture, and design. We are using high-quality components, cutting-edge signal processing methods and integrating hardware and software in a harmonic, compatible approach to ensure robust and stable performance for our users.

There exist five main blocks in our system. These are Transmitting Antenna Module, Receiving Antenna, Processing, Motor and Power modules.

Transmitting Antenna Module: This module is the target source that emits RF signals. Although this sub-system is not within our product, the design of the transmitted signal waveform and specification of the transmitting antenna is done by our team.

Receiving Antenna Module: This module can be considered as the RF frontend of the system. The RF signals are captured and fed through to the processing unit.

Processing Unit: Signal processing is done within this module. Control and decision-making algorithms are operating here.

Motor Module: This module is responsible for providing the necessary mechanical mobility to the entire system.

Power Module: Power module ensures the powering of components and sub-systems continuously and reliably

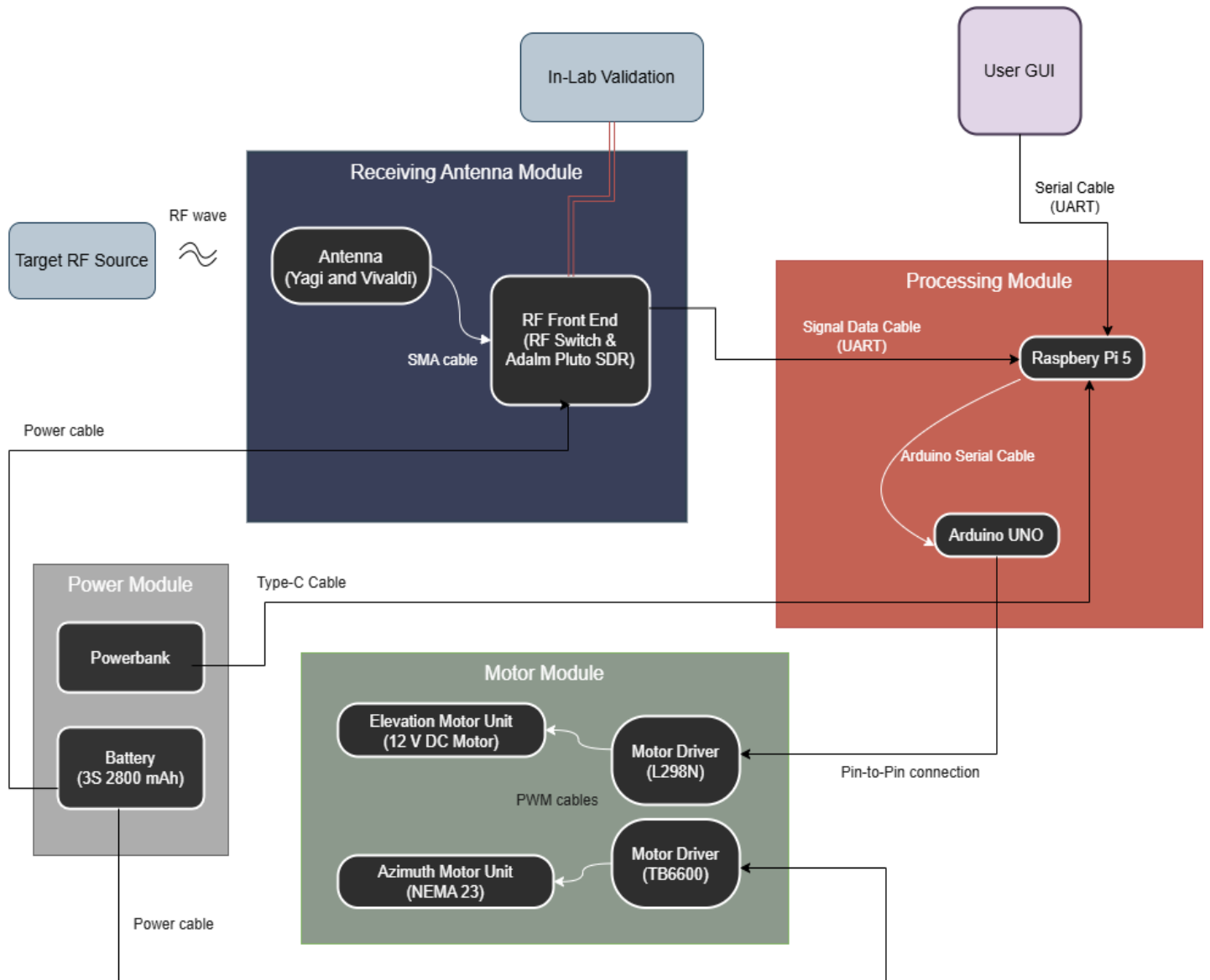


Figure 1: System and subsystem level block diagram

All the sub-systems are configured in a way that the communication and data transfer between them are at the finest quality and fastest speed the meet the system requirements. Moreover, compatibility of these sub-systems was considered by our team during the design process. As mentioned above, the sub-systems, their connections and the algorithms running within the modules arranged in a way so that the system can operate with the best performance. The figure 2 is a flowchart that describes the flow of the operation within the overall system.

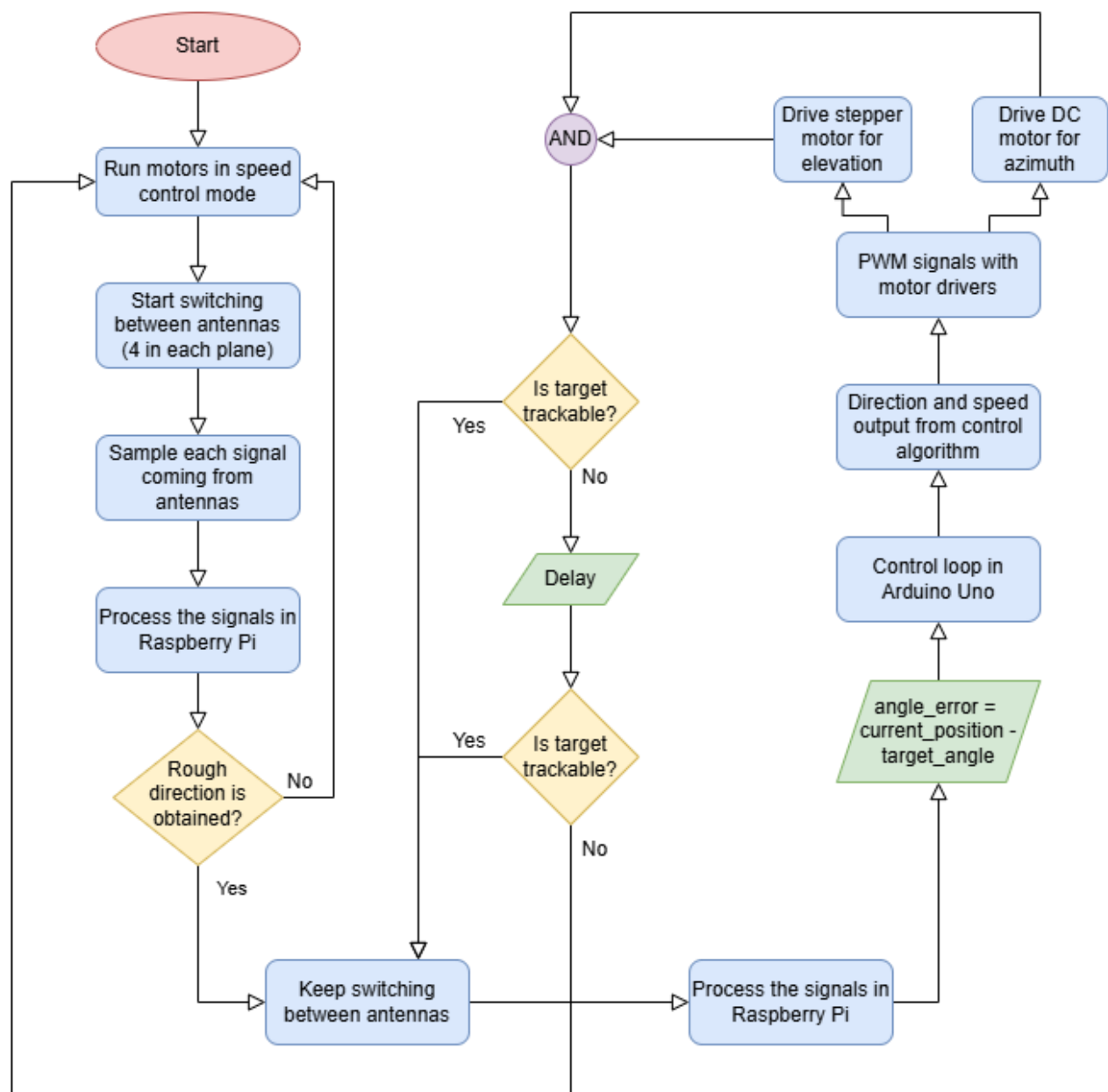


Figure 2: Working Principle in Flowchart Diagram

The flow of the operation consists of many checkpoints, caution and protection mechanisms and feedback loops to provide a stable and reliable operation. The main algorithm is also designed in a way so that the specifications and limitations of the hardware are considered and utilized in the most efficient way.

Technical Drawing and 3D Model

The one can observed 3D drawing of the finalized product in the Figure 3.

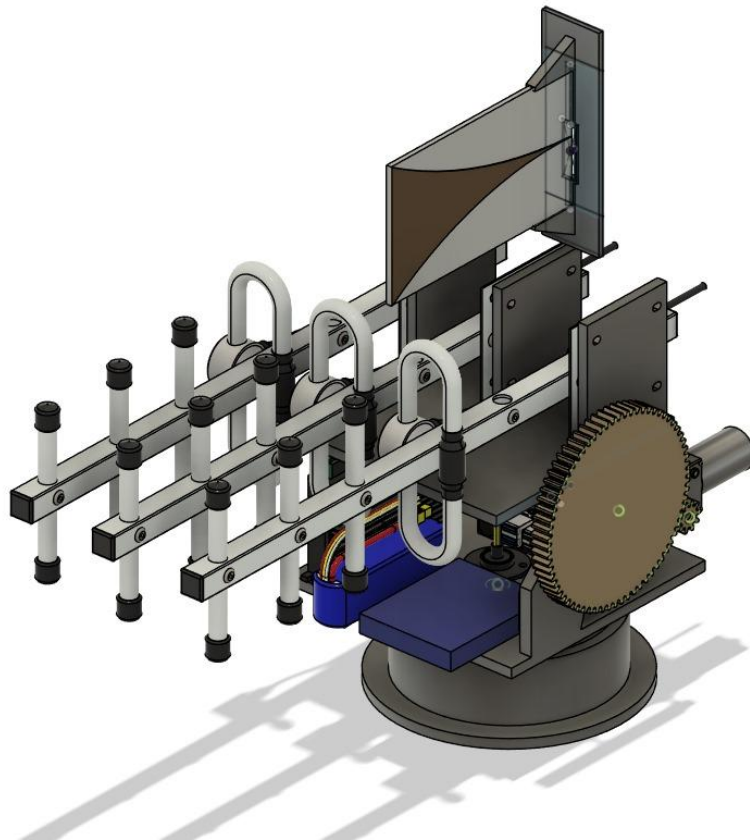
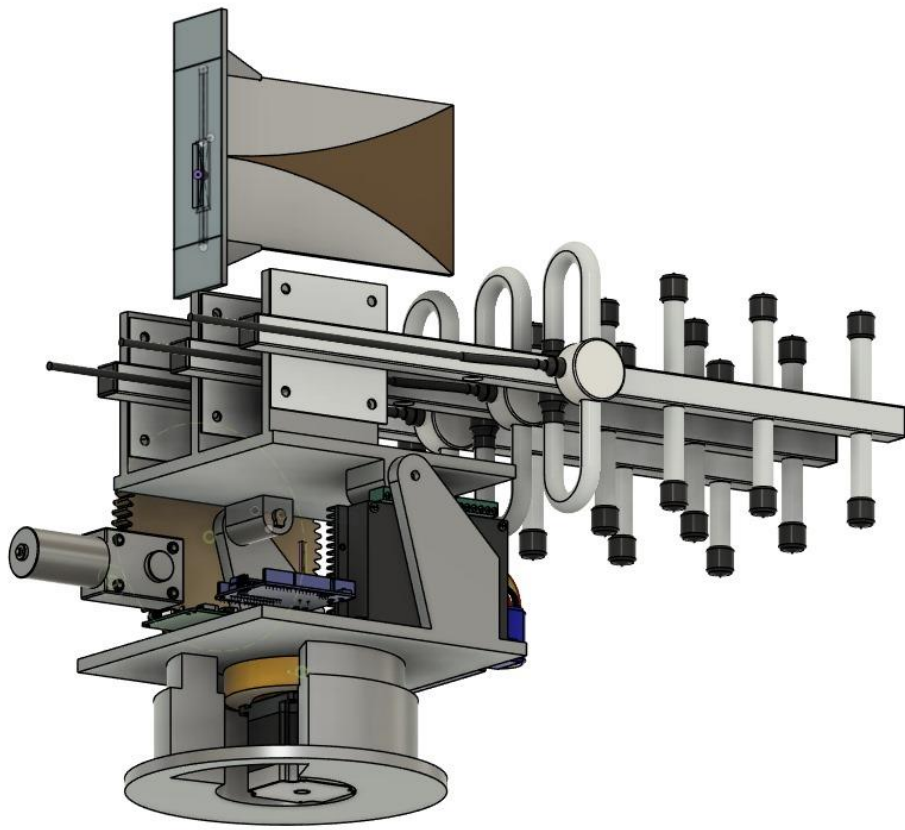


Figure 3: 3D Model of the finalized product

Subsystem Compatibility and Integration

Overall system is a complex, large-scale system. Therefore, integration of this system requires high precision of communication and data transfer and high caution. In this chapter, communication between subsystems, compatibility between them and how these sub-systems can form an operating overall system will be discussed. Through the development and integration of subsystems, reliable word-class standards (UART, etc.) have been followed.

Interface Analysis

Each subsystem is integrated through well-defined interfaces, with the Raspberry Pi 5 serving as the central processing hub that ties together the SDR, antennas, motor controls, and user interface. The Arduino Uno plays a critical role in real-time motor control, while the power and validation subsystems ensure that the system remains reliable and functional. By ensuring compatibility and efficient communication between subsystems, the overall system can autonomously track and maintain a line of sight with a moving RF-emitting target, delivering improved signal quality and power efficiency. To explain the signal and data transition, we define three main hubs: SDR, Raspberry Pi and Arduino Uno.

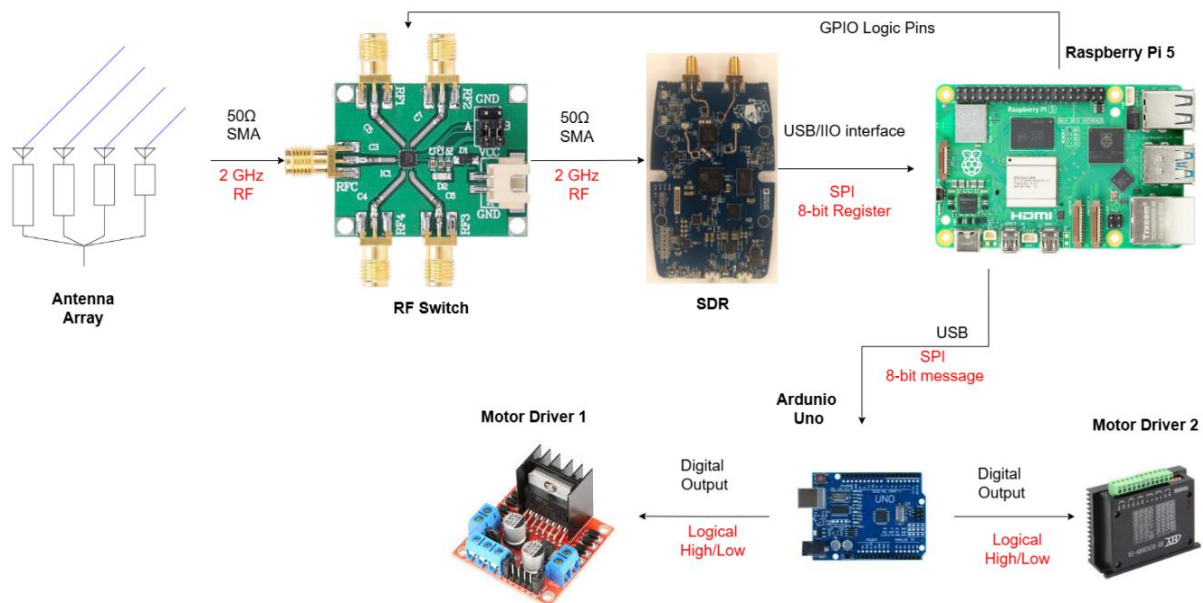


Figure 4: Interface Diagram

ADALM-PLUTO SDR

RF signals captured from antennas are connected to an RF switch. Antennas are connected to the RF switch with SMA cables and switch is logically controlled by Raspberry Pi. The RF output of the switch is connected to ADALM-PLUTO SDR via 50Ω SMA cables.

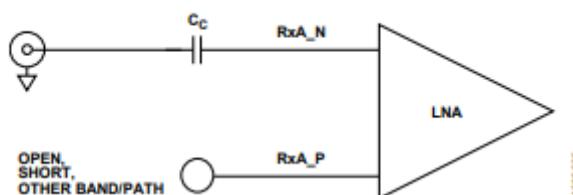


Figure 5: 50Ω Rx interface of SDR

The SDR converts the RF signals into digital signals thanks to its software-controllable RF components such as LNA, ADC, mixer etc^[1]. Due to the limitations of the ADC, RF signal level is selected and processed register is treated cautiously. The digital signal is then loaded into an 8-bit SPI register. The AD9361 outputs 8-bit register from its mini-USB port and then this port is connected to Raspberry Pi 5.

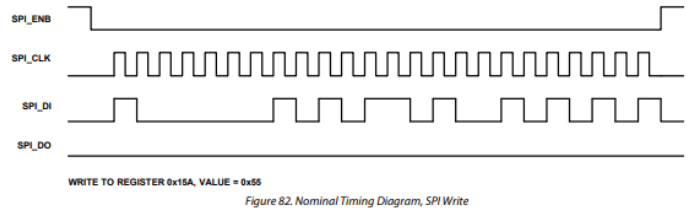


Figure 6: SPI output of AD9361

Raspberry Pi 5

The digitized RF analog signal is fed to Raspberry Pi 5. The AD9361 chip provides a driver^[2] developed by Analog Devices named “libiio”. Main script on Raspberry Pi 5 is selected as C++ to communicate with AD9361 chip from the operating system and execute signal processing algorithms converted from MATLAB. By using the mentioned driver, we can combine the digital signal fed to Pi 5^[3] with our signal processing functions in a script.

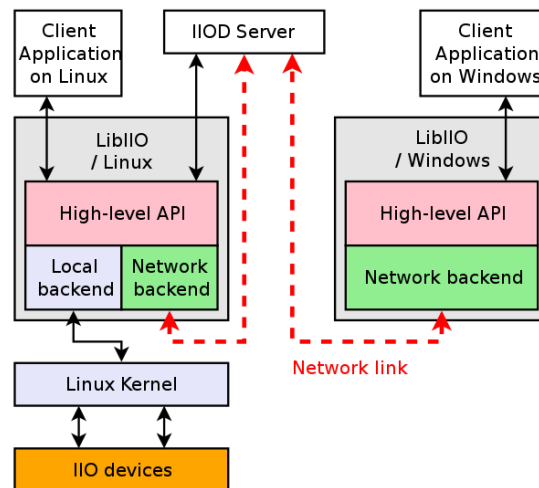


Figure 7: Interface of IIO device and Operating System

Moreover, the RF switch located in the RF frontend is powered by Raspberry Pi 5, 5V and GND outputs. The logic pins of the switch is controlled by the GPIO pins of the Pi 5. The logic pins are connected to a 2:4 TTL decoder and have an interface as shown below.

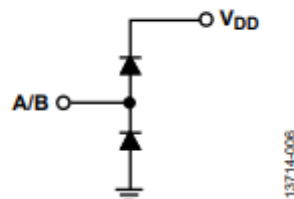


Figure 8: Logic control interface schematic^[4]

Finally, the Arduino UNO is also powered by Raspberry Pi 5 and communicating with it in a serial fashion. We are sending serial messages from our main script to the Arduino UNO which

then executes the controlling algorithm for the motors. The Arduino is connected to Raspberry Pi 5 with USB interface and receives 8-bit customized serial commands sent from the main C++ script.

Arduino Uno

Arduino Uno is connected to Raspberry Pi 5 with USB. It receives a serial message from the Pi 5 in a SPI fashion with a specified baud rate. Then this message is processed by the algorithm within the Arduino. The algorithm controls the digital output pins of the Arduino. These digital pins are connected to the two motor drivers TB6600 and L298N. The control logic in the algorithm determines the states of these logic output pins connected to motor drivers and in this way, Arduino can control the speed, direction and movement of the step and DC motors.

With this system architecture we can convert the captured RF signal into meaningful interpretable temporary data and then we can control the entire system. The data flow and transition of the data can be seen in the Figure 9.

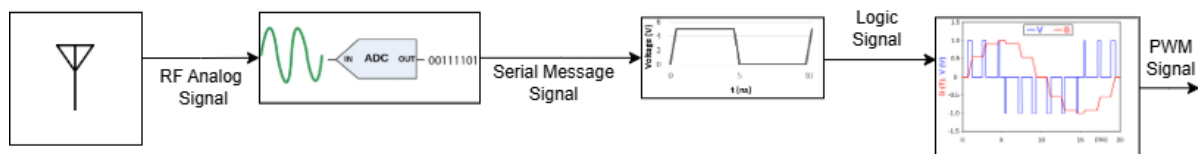


Figure 9: Flow and transition of data

Hardware and Software Synchronization

The AD9361 chip inside has its own reference clock to ensure a coherent reception between two ports. The data fed to Raspberry Pi 5 is in SPI fashion which has its own clock. The main script in Raspberry Pi 5 is written in C++. We ensure proper communication considering serial messages by providing necessary delays, callback and those kinds of implementations. Data logic voltage levels, fan-out problems are always considered and overcome with the current design to ensure a reliable data transfer. Moreover, drivers and libraries are installed with proper release dates to provide safe communication with peripherals along the system.

Subsystem Overviews

Transmitting Antenna Module

The transmitting antenna module consists of an ADALM-PLUTO SDR and an omnidirectional WIFI antenna that can work at a center frequency of 2 GHz. This module serves as a mobile RF source, transmitting a signal with a fixed center frequency to function as the target unit for the overall system. A primary design challenge for this module is designing the transmitted waveform to meet system-level requirements. The main algorithm used in the receiver module is Root MUSIC Algorithm. This algorithm assumes that all incoming signals are narrowband, so the phase difference across array elements can be modelled simply. Therefore, our prior choice of single tone sine works well with the algorithm. Thus, the transmitted signal has been chosen as a single-tone sinusoidal waveform. The operating frequency is carefully selected. Our Yagi-Uda antennas are actually cheap WIFI signal extenders and they are designed to work on the 2.4 GHz band. However, to not interfere with the WIFI band, we did S parameter measurements with VNA and found that our Yagi-Uda antennas are compatible with the 2 GHz band. Measuring that this is also compatible with our Vivaldi antenna at the top, it is decided to work on 2 GHz as a center frequency.

Receiving Antenna Module and Angle of Arrival Estimation

The updated passive direction-finding system uses a dual-channel Pluto Software-Defined Radio (SDR) in conjunction with a hybrid antenna configuration to estimate the direction of arrival (DoA) of radio frequency (RF) signals in both azimuth and elevation domains. This system is designed for enhanced angular resolution while maintaining a simplified hardware architecture, using a combination of sequential sampling, correlation-based signal alignment, and subspace-based spectral estimation techniques.

The antenna subsystem consists of one central Yagi-Uda^[A1.1] antenna connected directly to Pluto SDR Channel 1 (common reference antenna), an SP4T RF switch, controlled in real time to alternate Pluto SDR Channel 2 between, Left Yagi-Uda antenna, Right Yagi-Uda antenna, Vivaldi antenna (top-mounted). This hybrid architecture enables spatial sampling in both the azimuth and elevation planes using a minimal number of RF receivers and ADCs.

The azimuth plane is scanned using a three-element Yagi-Uda phased array:

- Left Yagi (connected via switch)
- Middle Yagi (directly connected to Channel 1)
- Right Yagi (connected via switch)

Elevation angle estimation uses:

- The same middle Yagi (common element)
- A top-mounted Vivaldi antenna, connected via the SP4T switch

The azimuth antennas are aligned horizontally and form a linear uniform array along the x-axis. In ideal conditions, the phased antenna array structure requires coherent sampling to accurately estimate the direction of arrival. However, due to the excessive cost of adding additional coherent SDR channels, we followed a different approach using RF switches and two coherent receive channels of the ADALM-Pluto SDR. Unlike traditional systems that perform simultaneous sampling across all antenna elements using multiple synchronized channels, this design uses a sequential acquisition scheme to reduce hardware complexity.

In Azimuth sampling, first, the SP4T switch connects the left Yagi, and samples are captured from left and middle antennas. Then the SP4T switches to the right Yagi, and samples are captured from right and middle antennas. During operation, each switching cycle generates partial data corresponding to two antenna pairs. To reconstruct the full three-element coherent snapshot, a temporal alignment step is performed. Accurate Angle of Arrival (AoA) estimation requires coherent antennas. However, Sequential sampling introduces phase discrepancies due to non-simultaneous acquisition. To tackle this, the system implements calibration and signal alignment via cross-correlation techniques

The common antenna (middle Yagi) is sampled in all configurations and is connected to one receiver channel of the SDR all time. Using the repeated signal from the common antenna, cross-correlation is performed between adjacent acquisition windows to estimate the relative delays. Based on these offsets, a time-alignment correction is applied to simulate simultaneous signal snapshots across the antenna array.

After these operations, elevation sampling is performed. The SP4T switches to the Vivaldi antenna, and samples are captured from both Vivaldi and middle Yagi antennas. In this configuration, the temporal alignment is not applied since ADALM-Pluto receiver channels are enough for two coherent measurements.

Angle of Arrival Estimation

After alignment and sampling, each plane (azimuth and elevation) is treated as a linear sensor array. The system employs the Root-MUSIC (Multiple Signal Classification) algorithm for high-resolution AoA estimation.

For azimuth scanning, a 3-element linear array (left, middle, right Yagi antennas) is reconstructed. The signal covariance matrix is estimated from aligned samples. Root-MUSIC computes the eigen structure of the covariance matrix and identifies the signal and noise subspaces. The roots of the array polynomial on the unit circle are evaluated, and the angles corresponding to the minimum orthogonality to the noise subspace are selected as the AoAs. This provides high-resolution estimates, particularly when the signal-to-noise ratio is sufficient and inter-element spacing is appropriately chosen (typically half-wavelength).

For elevation scanning, a 2-element vertical array (Vivaldi and middle Yagi) is used. The same Root-MUSIC framework is applied in one dimension to resolve elevation angle. Due to the reduced number of elements, the elevation scan resolution is not as good as the azimuth but is sufficient for the requirement of the project.

Processing Module

The processing modules mainly consists of two units, which are Raspberry Pi 5 and Arduino Uno. Below, these two units are elaborated separately.

Raspberry Pi 5 (Main Processor) The Raspberry Pi 5, “work machine”, is responsible for capturing signal samples from the SDR/antenna module, processing them (using C++), and determining the target angle. Its main tasks are listed below.

- Perform angle-of-arrival and signal strength computations.
- Communicate with a GUI that provides real-time system monitoring.
- Send the calculated angle commands to the Arduino via a serial bus.

The digital signal processing methods which is utilized for the methods described previously is now running within a C++ implementation on Raspberry Pi 5. Our main method uses a correlation method between the captured and sampled signals in order to extract the phase difference information. This phase difference information is then converted to an interpretable data for the control system. The processing module works in the similar fashion as we explained previously. Only difference is, now our processing algorithm is completely converted to C++. Therefore, all the signal analysis and serial communication will be done on C++ scripts.

Arduino Uno (Control Loop)

Arduino executes the low-level, real-time control of the motors. It receives angle targets from the Pi and drives the motor module (e.g., stepper or DC motors) to the correct orientation. Below are the main tasks of Arduino Uno.

- Interface with motor drivers through PWM, direction, and enable lines.
- Implement a control algorithm to ensure fast and precise aiming.

The communication between the Raspberry Pi and Arduino is employing UART interface using the Serial Bus. The Arduino can respond with status updates. For the communication between the RF Front End and Pi, communication is happening over USB. In our trials, we have seen the USB connection can create communication fast enough to provide a healthy control.

Why choose a Two-Controller Setup?

- **Real-Time Motor Control:** The Arduino's dedicated microcontroller architecture ensures consistent timing for motor pulses, avoiding Linux scheduling delays.
- **Task Separation:** The Pi handles computationally intense signal processing and the GUI, while the Arduino focuses on stable, low-level control.
- **Hardware Compatibility:** Arduino has abundant libraries and shields for motor control and sensor reading, speeding up development.
- **Fault Protection:** In case of an electrical fault from the motor module side, the worst scenario would be losing the Arduino which is extremely cheaper compared to Pi.

We ensured that the SDR connection to the Raspberry is over USB Serial Port. With another port being occupied by Arduino.

Motor Module

1. Motor Selection and Mechanics

The range of motion of NEMA 23 stepper motor is full 360° rotation. Its step size is 1.8° per full step. With microstepping we achieved a 0.225 step size. It allowed our motor to rotate in a more precise and controlled manner. The controller employs a linear acceleration and deceleration profile. Below are the several reasons behind this stepper motor choice.

- NEMA 23 typically offers high positional accuracy and holding torque (often in the 1–1.5 N·m or more range), making it top preference for larger antenna assemblies.
- No mechanical stops, enabling a full 360° sweep and a continuous motion.

In the horizontal rotation, we have designed and implemented a 3:1 ratio ring gear. The upper body is mounted on a 60mm inner diameter bearing. The motor will rotate the inner gear on the side. This setting will allow us to place slipper ring in the middle of rotation which transmits the motor and GUI cabling to ground level.

We have been employing the servo motor with a 12V 18 RPM DC Motor in elevational rotation. It has a holding torque of 39 kg/cm ensuring the movement capability on the elevation axis when combined with a 7:1 ratio gear. The range of motion is -55° to +45° in this application. The active torque applied by the system changes as it rotates on the motor axis.

2. Motor Driver and Power Supply

In horizontal rotation, the TB6600 offers improved performance, especially in applications requiring precise control. It supports microstepping, which allows for smoother and more accurate motion control of the stepper motor (NEMA 23). The advantages of TB6600 are as stated below:

- Microstepping support for higher precision and smoother motion.
- Better heat dissipation and current control capabilities, which are more suitable for the operational demands of the stepper motor used.

The L298N is used to drive the DC Motor on the side for the elevation movement control. While the L298N lacked features required for driving a stepper motor, it is an effective choice for driving the 12 V DC motor on the side. The Arduino library for the L298N allows us to easily implement a control algorithm for driving the DC motor.

To support long operation times, the 3-cell Li-Po battery with 2800 mAh capacity is used. It nominally supplies 11.1 V (3.7 V per cell), reaching up to ~12.6 V when fully charged. Both the stepper motor and the DC Motor draw power from this Li-Po source.

To ensure battery health and prevent over-discharge, a voltage tester module is attached to the Li-Po continuously monitor cell voltages throughout operation.

3. Control Logic and Speed Requirements

The speed requirement is at least $15^\circ/\text{s}$ to track rapidly moving targets. We have also achieved similar results on the elevation module with a high ratio gear implementation.

Stepper motor control loops will function as listed below.

- The Raspberry Pi calculates the desired azimuth angle error and sends it to the Arduino.
- The Arduino's controller algorithm adjusts the step rate (and direction) for the motors.
- The position feedback comes from the antenna module. Therefore, we have a speed control based on position feedback.

In the opening scenario, the system starts searching the target by rotation in the horizontal axis with constant speed. This pre-defined scenario allows system to find the target under 3 seconds. As soon as the target is detected, the tracking algorithm starts to operate.

The horizontal motor control for tracking is implemented with a PI controller. On polar plane, its active zone consists of $\pm 30^\circ$. The PI controller allows a smooth control inside this region. Outside this region, speed is saturated with its maximum value. This maximum value is well over the speed requirement of horizontal tracking and allows system to quickly catch the target. This PI controller allowed the system to track the target without an overshoot.

The 12V 18 RPM DC motor, known for its high holding torque, is well-suited for handling elevation adjustments with both stability and sufficient speed. Its rotational capability allows it to cover typical angular ranges within a practical time frame, while maintaining the force needed to hold position under varying loads.

The Arduino controls the motor through PWM signals, adjusting the duty cycle in real time based on the error. Additionally, the control logic accounts for torque variation during elevation changes (for instance, when the motor must work against gravity at steeper angles or stabilize under shifting loads). By dynamically adjusting the power input in response to changing torque demands, the system ensures consistent motion and prevents stalling or overshooting. Fine-tuning achieved smooth acceleration and deceleration, avoiding oscillation while maintaining precise control throughout the motor's movement range.

Both motors are sized to handle the weight of the antenna assembly plus additional components (e.g., cables, protective housing). The NEMA 23 is often rated for moderate torque (e.g., $1.0\text{--}1.5\text{ N}\cdot\text{m}$) which is sufficient for rotating a small to medium antenna array if the assembly is balanced. DC motor can handle moderate loads (torque $\sim 39\text{ kg}\cdot\text{cm}$). After a high number of trials, we could achieve a speed of $\sim 28\text{ rpm}$, meaning $168^\circ/\text{s}$ on horizontal rotation. This is achieved thanks to the ring gear and bearing combination.

Power Module

The power module supplies energy to the RF switches in addition to the stepper motor and Raspberry Pi 5. Given the high current draw of the power module, thicker, heat-resistant cables is used to ensure safe and efficient power delivery. This minimizes the risk of overheating and voltage drops, preserving the stability of the system during extended operation. To maintain continuous performance, the Li-Po battery and power bank levels must

be regularly monitored and recharged as needed. Ensuring these power sources remain sufficiently charged prevents interruptions in system operation. Additionally, careful attention is given to the power cable connections to avoid loose or faulty wiring, which could disrupt the power flow or damage sensitive components. Overall, effective power management and proper cabling is essential to maintain system reliability and to prevent power-related failures during operation.

Computer Controlled Signal Emulation and In-Lab Validation Subsystem

To evaluate and verify the functionality of the passive direction-finding system under controlled conditions, a laboratory-based signal emulation framework is integrated into the design. This subsystem allows rigorous testing of the azimuth and elevation estimation algorithms without relying on external over-the-air RF transmissions or physical antennas. The goal is to enable reproducible, high-fidelity simulations of angular trajectories by injecting known signals directly into the receive paths of the system.

In this test configuration, the antenna elements are replaced with direct coaxial cable connections to the Pluto SDR receiver. A calibrated signal generator is used to emulate the received RF wavefronts corresponding to desired AoA trajectories. The system components involved include ADALM-Pluto SDR Channel 1 and 2 connected via SMA coaxial cables to the signal feed, representing the antennas. This setup allows software-controlled injection of signals that mimic the relative phase and amplitude shifts experienced by spatially distributed antennas for arbitrary source trajectories.

A graphical user interface (GUI) is developed to simulate a moving signal source across both azimuth and elevation planes. Users can determine error. The GUI synchronizes signal emission across the relevant ports using the additional SDRs for transmission (signal generator). The signal generator applies these phase shifts to its outputs to simulate a wave arriving from a specific direction. The result is a time-varying signal injection sequence that corresponds to a moving RF source, emulating realistic AoA patterns.

Graphical User Interface

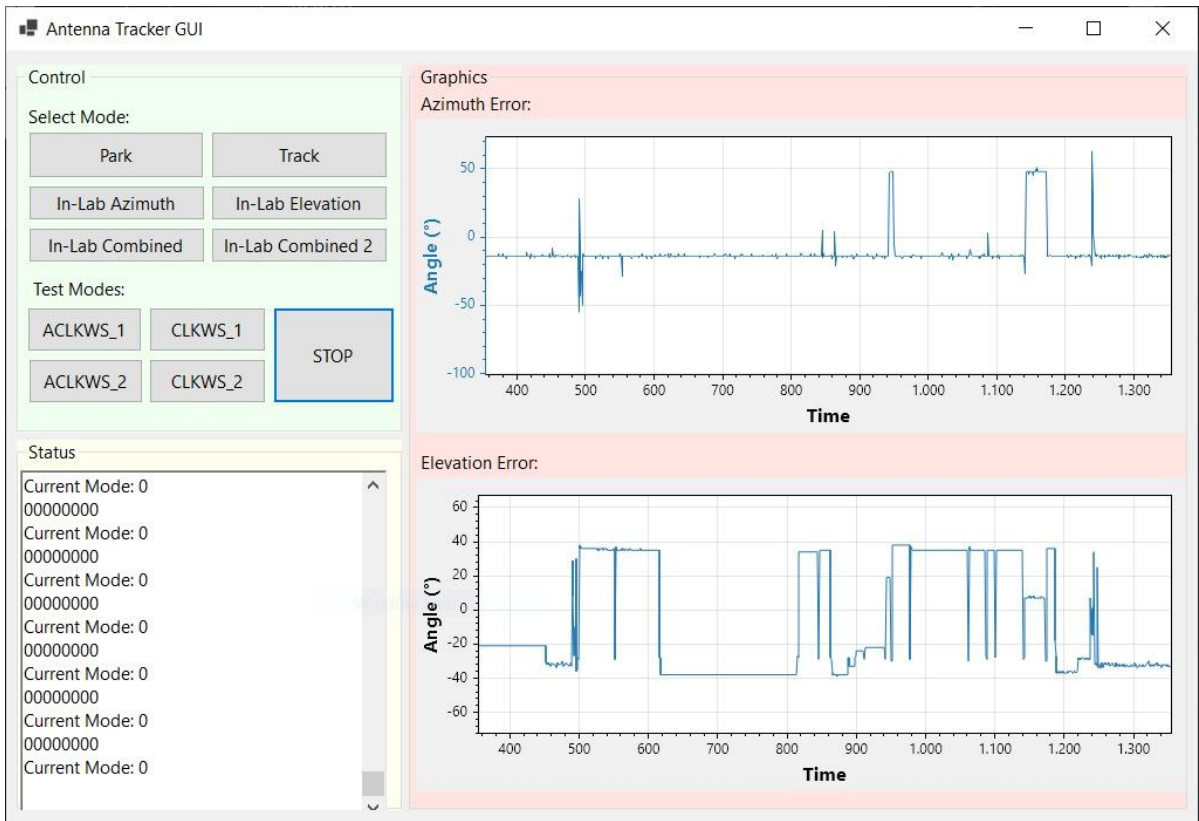


Figure 10: Antenna Tracker GUI

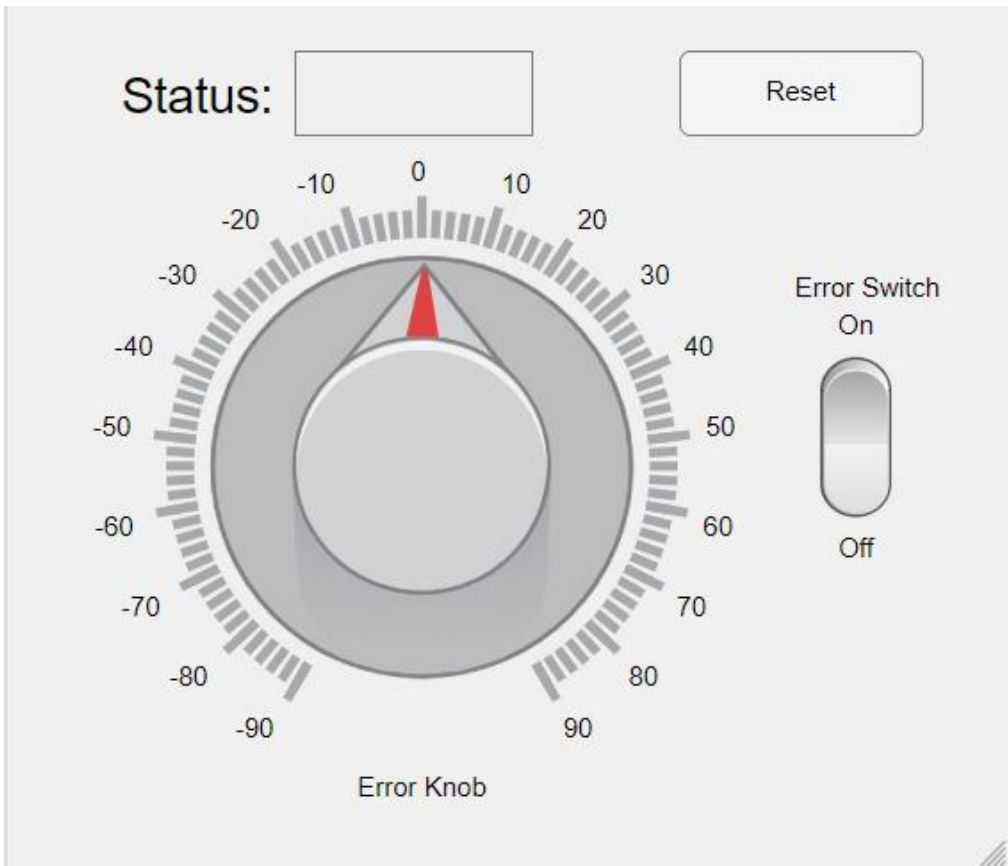


Figure 11: In-Lab Validation GUI

To enhance usability and ensure seamless interaction between the user and the system, a Graphical User Interface (GUI) is developed using C# as shown in Figure 10. This desktop application serves as the primary interface for controlling and monitoring the device. Communication between the GUI and the embedded system is established through a UART (Universal Asynchronous Receiver-Transmitter) serial connection, allowing for reliable, real-time data exchange.

The C# GUI offers a range of essential functionalities, including mode switching: Users can toggle between different operation modes, such as manual control, automated tracking etc.

The GUI is designed with a clean, intuitive layout to ensure accessibility for users of varying technical backgrounds. Its UART-based communication ensures efficient command delivery and data retrieval, making it a reliable bridge between the user and the underlying hardware.

Compatibility with Requirements

Table 1: Compatibility Table

Requirement	Design Decision	Compliance Justification
Constant center frequency operation	Transmitter operates at 2 GHz with single-tone sine wave	Ensures narrowband assumption validity for Root-MUSIC; avoids Wi-Fi interference while staying within antenna operational range
Tracking lock-in within 3 seconds	Fast data acquisition via coherent subarray and fast processing time using C++ High constant speed mode when target is not detected	Using C++ enables fast processing time, which results in approximately 5 angle measurements per second. Constant speed mode allows the system to quickly scan the area and find a rough result.
RMS angular error < 5° after lock	Root-MUSIC algorithm with 3-element azimuth array and calibrated alignment Microstepping with motor driver	High-resolution AoA estimation with subspace methods provides fine angular resolution Microstepping has allowed motor to move with much smaller discrete steps providing more precision

Track target moving at $\geq 15^\circ/\text{s}$ in azimuth	A ring gear design mounted on a bearing with 3:1 ratio	A speed of $180^\circ/\text{s}$ is achieved in azimuth during speed tests
Resilience to single-source jamming (100 kHz, -80 dBm)	Narrowband signal with temporal correlation; Root-MUSIC focuses on spatial signal structure	Narrowband high-SNR processing reduces jamming impact; common antenna acts as a stable reference
Modularity & compactness	Using only 2-channel SDR and an RF switch reduces hardware count.	Ensures hardware simplicity while enabling spatial sampling in two dimensions

Discussion of Engineering Trade-offs

Hardware Cost vs. Sampling Coherency: Coherent AoA estimation typically requires multiple synchronized receivers. This design uses a cost-effective alternative—RF switch and dual-channel SDR—with post-acquisition alignment via correlation. While this requires temporal calibration and may worsen the measurement slightly, it avoids the cost and complexity of multi-SDR coherence.

Azimuth Resolution vs. Elevation Capability: The system prioritizes azimuth accuracy by allocating three elements to azimuth and only two to elevation. This results in slightly lower elevation resolution, which is acceptable as the elevation requirement is less stringent.

Choice of Lesser Antenna: Choosing 1 additional antenna for the elevation reduces the antenna number but brings lesser precision in elevation measurements. Adding one more antenna may increase precision but may conflict with modular design

Jamming Resilience vs. Signal Design Flexibility: A single-tone waveform is less flexible than wideband or spread-spectrum signals for hybrid approaches but maximizes SNR for the Root-MUSIC algorithm and allows easier correlation-based temporal alignment. It satisfies jamming constraints by being narrowband and coherent.

Compactness vs. Speed: The implementation of DC motor for elevation movement brings up a much more resilient system. But the DC motor is pretty bulky and heavy compared to the servo motor. For now, our choice is the DC motor, but further tests will confirm the final decision.

Simple Design vs. User-Friendliness: To build a user-friendly easy-to-use system, we had to come over some design complexities such as adopting a mechanical design to place a slipper ring in order to deliver a cable-connected reliable GUI connection. We also needed to come up with some tricky solutions in order to tackle the mechanical flaws such as disturbing noises etc.

Test Procedure

To evaluate the performance and reliability of the RF-Based Antenna Tracker system, a series of in-lab and outdoor tests were conducted under control and operational conditions. Prior to each test, the power sources of both the Raspberry Pi (powered by a 10,000 mAh powerbank)

and the motor system (powered by a 3-cell LiPo battery) were checked. The Raspberry Pi was accessed via VNC from a local computer, and the main executable was launched. A USB serial cable was used to connect the antenna tracker hardware to the system. The graphical user interface (GUI) named “antenna_tracker” was then initiated, allowing the user to select between different test modes. For in-lab validation, the “in-lab validation” mode was chosen to manually test the system’s responsiveness. Offset values were adjusted using physical knobs, and the tracking process was activated by flipping a switch. Once the system began rotating, a stopwatch was started, and the elapsed time was recorded when the system successfully reached and stabilized within a $\pm 5^\circ$ range of the target angle. For outdoor target tracking, the procedure followed similar initial steps, but the “tracking mode” was selected from the GUI. After the system successfully locked onto the RF-emitting target, the target was repositioned to various random locations at distances of 1 to 5 meters. Tracking errors in both azimuth and elevation axes were then measured using a tape measure and calculated with trigonometric methods based on the distance and the angular displacement between the target and the midpoint of the receiver antennas. Throughout the testing process, angular arrival durations and tracking errors were compared to expected benchmarks to verify whether the system met the required performance thresholds under dynamic conditions.

Test Setup



Figure 12-13: Test Environment

We conducted several tests to measure and observe the system level requirements of our products.

- Search Test
- Tracking Performance Test
- Azimuth Tracking Error
- Elevation Tracking Error

We all noted the errors in an RMS fashion by conducting the same test at the very same test point for sufficient times.

Search Test

Goal of this test was to observe the search system performance which locates the target upon the start of the system whose location is unknown. We also measured the time elapsed until the detection of the target. We repeated the test for different distances and initial locations of the target.

Tracking Performance Test

Main goal of this test was to measure the arrival time of the system at the target located at the desired angle. We wanted to test the requirement of the system.

Tracking Error Tests

Main goal of these tests were to observe and measure the accuracy and the precision of our direction-finding system and algorithm. We observed the $\pm 5^\circ$ error margin compatibility and direction-finding performance of our system.

Results and Evaluation

We have collected several measurements for each step in order to calculate our error in RMS. For the error calculation, we compared our ground truth time value with measured time. The plots regarding the measurement and ground truth can be seen below.

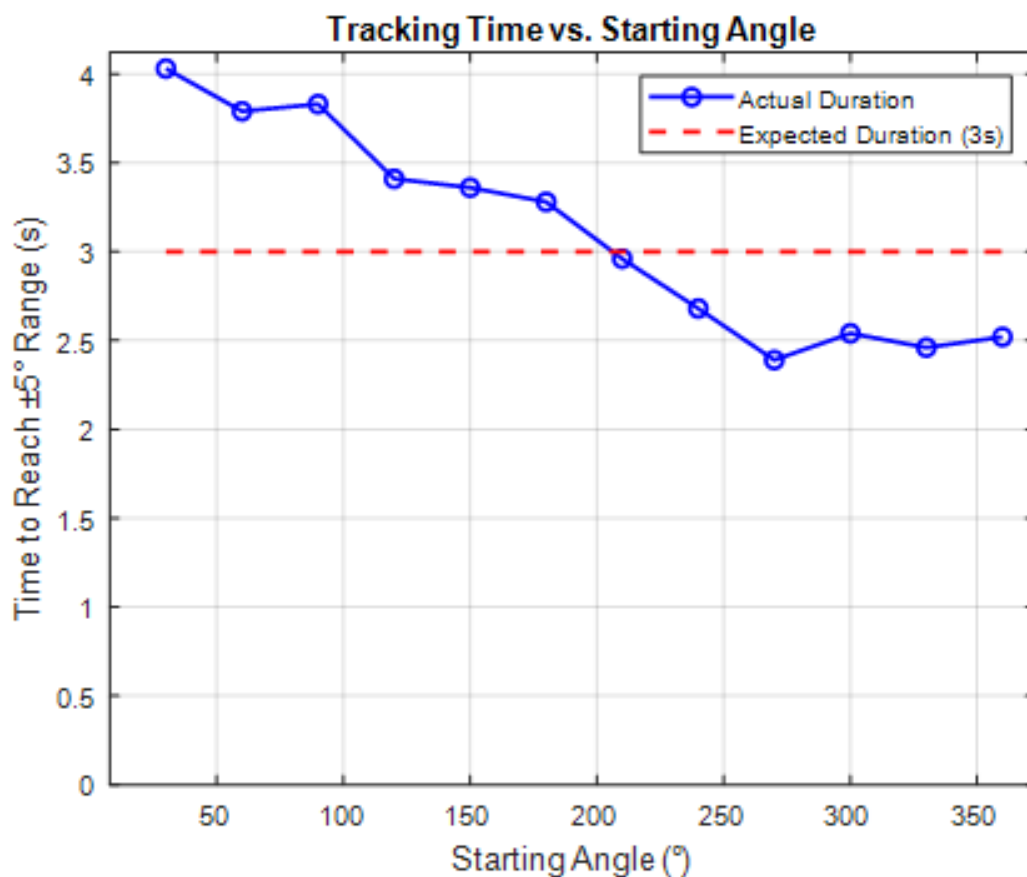


Figure 14: Test results – Search test

For the next test, we measured the time elapsed for our system to be aligned with the target when the target was fixed to different angular positions with respect to our system.

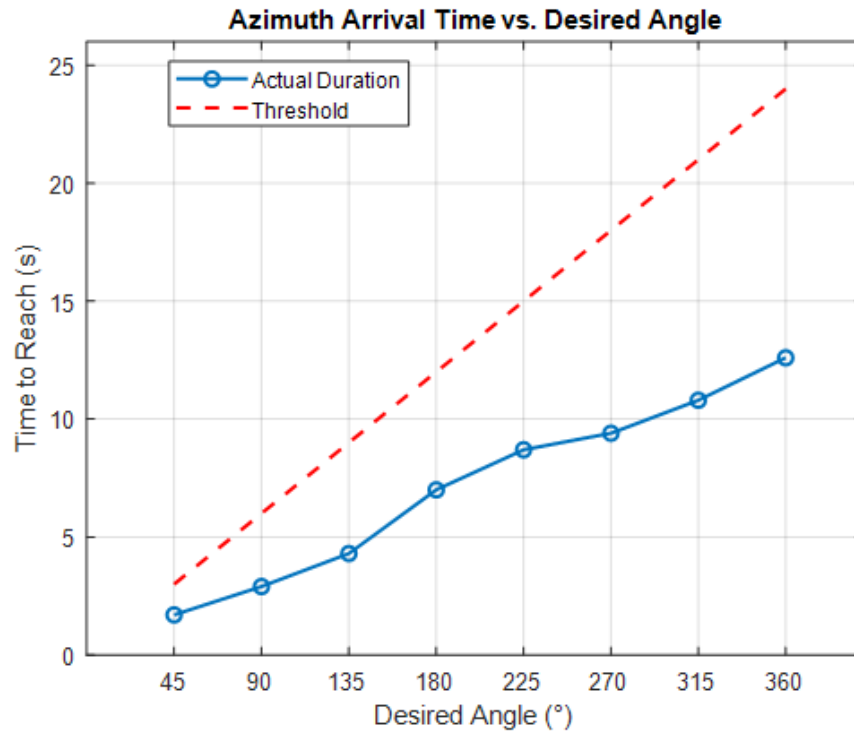


Figure 15: Tracking performance test

The test results indicate that our system is able to track the target within the error margins.

To be able to observe the tracking performance and observe the direction finding precision of our system, we conducted two more test locating the antennas to predefined positions and measuring the error between the tip of the cen"ter antenna and the target transmitter.

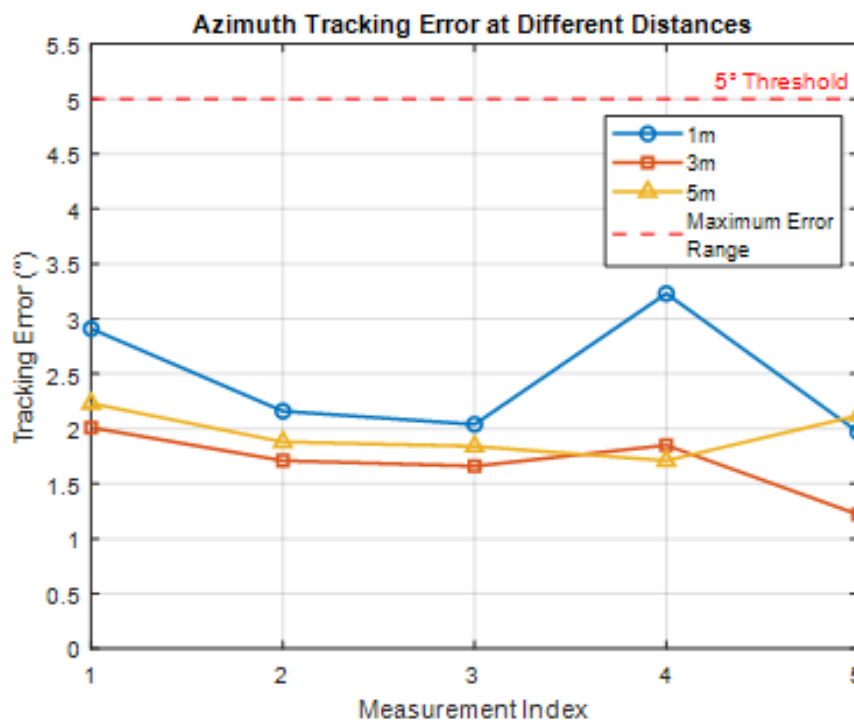


Figure 16: Test results – Azimuth tracking

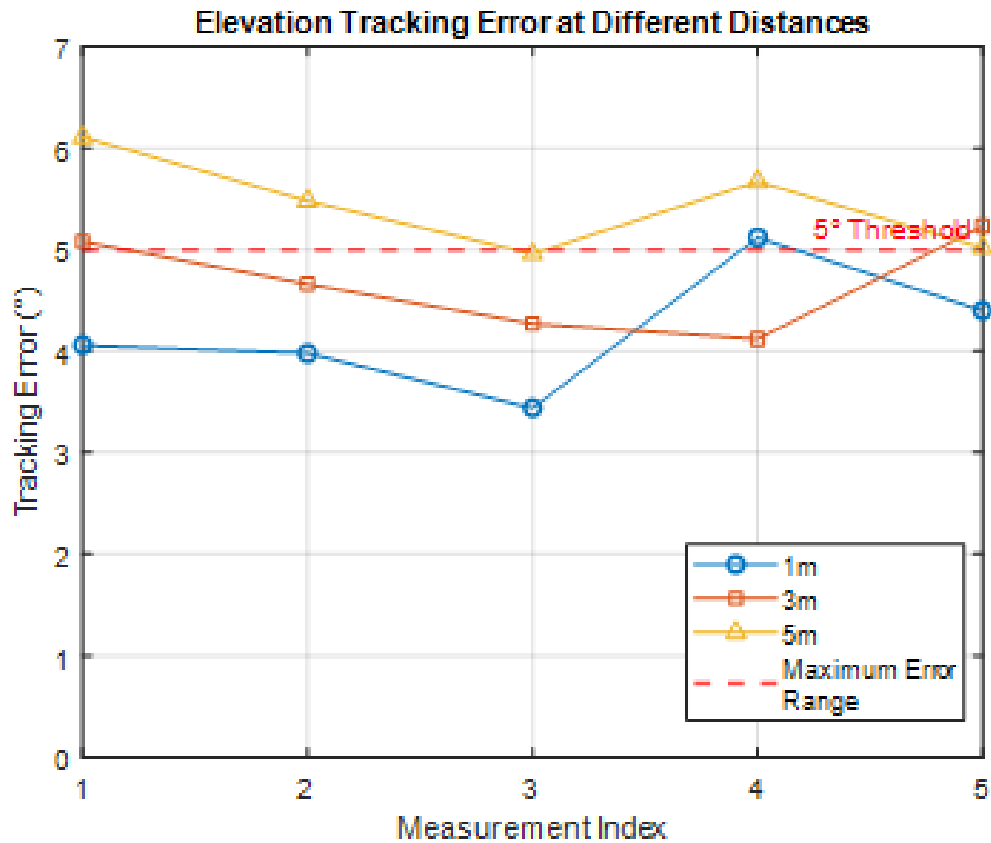


Figure 17: Tracking performance

The tracking error is calculated for 5 different points for different distances. Here from Figure 16 and Figure 17 we can see that most of our measurements are within the error range. The meaning of all measurements are way below the error limit.

The tests mentioned were conducted with caution and measured with precision. All procedures, parameters and test setup are covered in detail in test procedure documents, which can be found in Appendix A2.

Resource Management

We divide our resource allocation into to main parts namely, cost and power allocation.

Cost Analysis

Table 2: Cost Analysis Table

Component	Single Cost	Amount	Total Cost
NEMA-23 Stepper Motor	14.56\$	1	14.56\$

12 V DC Motor with Gearmotor	10.49\$	1	10.49\$
Raspberry Pi 5	102.47\$	1	102.47\$
Arduino Uno	4.93\$	1	4.93\$
HMC7992 RF Switch	8.94\$	1	8.94\$
ADALM-PLUTO	200\$	1	Subsidized
L298N Motor Driver	2.05\$	1	2.05\$
TB6600 Motor Driver	10.3\$	1	10.3\$
3D Filament	14.89\$/kg	400 grams	5.95\$
Slipper Ring	12.77\$	1	12.77\$
SMA Cables	5.12\$/m	5 meters	25.6\$
u.FL to SMA Cable	3.2\$	1	3.2\$
FR4 Copper Plaque	1.43\$	1	1.43\$
2.4GHz Yagi-Uda Antenna	9.75\$	3	29.25\$
3S Li-Po 2800mAh Battery	15\$	1	15\$
TOTAL ESTIMATED COST			246,94\$

In general, our product breakdown consists of the motor structure, RF frontend components, structural frame components, processing components, and some middle components such as

cables. After selecting a component, we compared the existing models in the market from cost and specifications point of view. We often bought a single sample to test and ensure the performance and compatibility of the component in our system before purchasing them as an whole.

During the product selection, as a team we paid attention to select the high-quality products which can affect the performance of the overall system. We bought a high-power processor to implement complex signal processing algorithms. Moreover, to handle the weight of the system and to ensure the desired mobility, we selected motors with sufficient figures of merit. Middle components such as cables or drivers were selected according to our budget. As a team, we adopted a mentality such that our main goal was not only to build an operating system but also build it in a cost-effective approach.

Power Analysis

The main components that consume significant power are Raspberry Pi 5 and motors. Motor unit is powered by a Li-Po battery. We separated the power units for the motor and other modules to ensure high power for the mobility unit and to not distort the processing power. The other modules are powered up by Raspberry Pi. Only the switch and SDR receive power at the receiver module as antennas are passive. We also power up the Arduino, which runs the control algorithms from Raspberry Pi

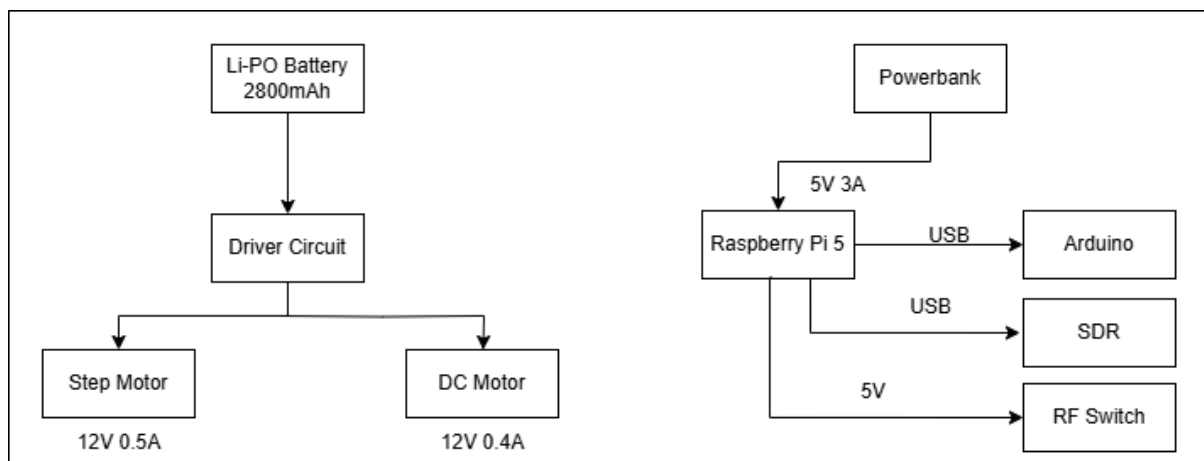


Figure 18: Power Distribution Diagram

Table 3. Maximum power consumption

Component	Max. Power Consumption
Step Motor	~24W
DC Motor	~24W
Raspberry Pi 5	~7.5W

Table 3 maximum power consumption of the components that consume the most power. However, the design will never use the maximum rated values for power consumption. Therefore, by estimating an average torque for motors, considering the ratings of our battery units we can estimate power consumption.

Table 4. Average power consumption

Component	Max. Power Consumption
Step Motor	~6W
DC Motor	~4.8W
Raspberry Pi 5	~5W

In table 4 and Figure 14, one can observe the average power consumption of the previously mentioned components. The average power consumption is calculated as ~12.25W. Datasheets ^{[5],[6]} of the components were utilized for this calculation.

For runtime calculations, we considered average values (a total current around 1A), and our calculations yielded that the current power configuration is sufficient for a stable and lasting operation of the system. Moreover, we have done numerous tests such as powering the system and measuring the battery levels periodically. Those results show that the current selection of power units meets the demands.

$$\frac{2800 \text{ mAh}}{1A} = 2.8 \text{ hours}$$

Equation for nominal runtime calculation

Several tests were conducted to observe power consumption. We measured how much time it takes for the battery to reach %75 level.

Table 5. Battery level test results

Test	Time
Idle Mode	100-120 Minutes
Operating Mode	75-90 Minutes

In the event of performance degradation of Raspberry Pi 5 due to unstable electrification, we are going to replace the power bank with a battery unit by using a proper voltage regulator (5V in our case). This minor modification is going to be done if such happens during further tests.

Schedule Analysis

An updated project schedule with a Gantt chart is provided to reflect the latest timeline and progress of the project. As of the Critical Design Review phase, the development is proceeding according to plan. While some phases required timing adjustments due to design changes and real-world constraints, these were managed without jeopardizing the final delivery.

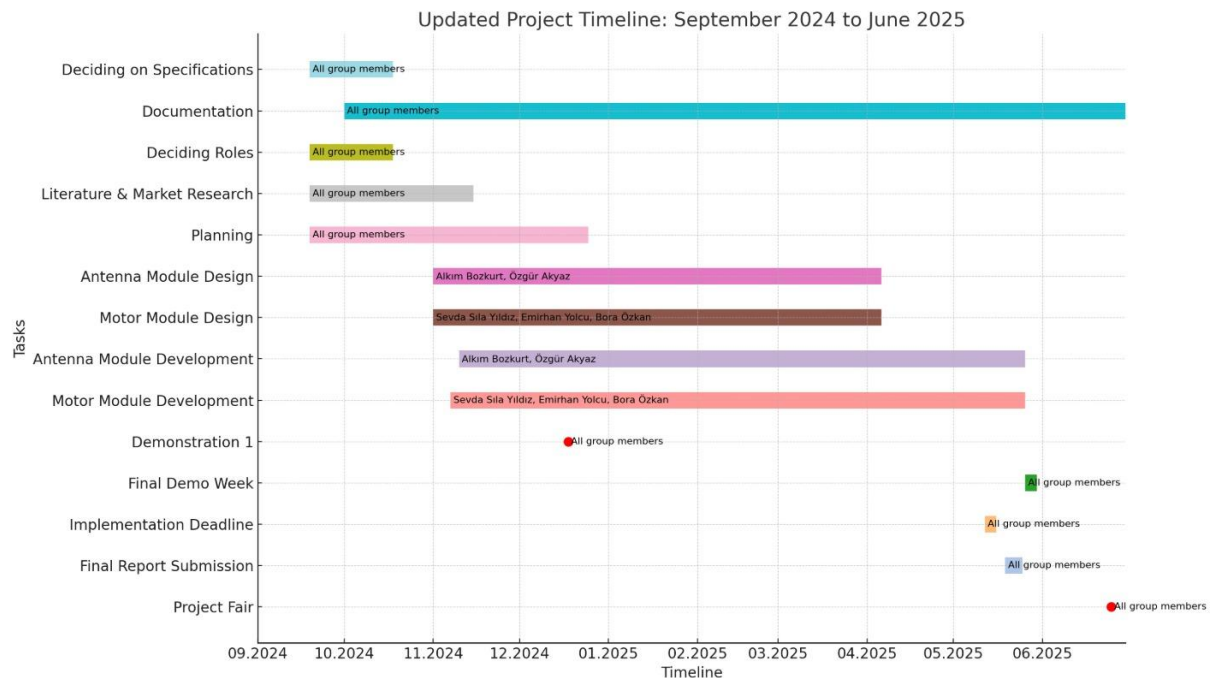


Figure 19: Time Schedule of Our Team Gantt Chart

There were periods when progress slowed temporarily, mainly due to component shipping delays and 3D printing lead times. Although these instances did not cause significant delays, they did limit available workdays. During those times, efforts were shifted toward software implementation, integration planning, and system documentation to maintain momentum.

One important change during this period was a shift in the signal processing implementation. The initial idea to use MATLAB for embedded processing was reconsidered, and the algorithms were restructured in a more lightweight environment. This adaptation ensured smoother integration with the rest of the system and better compatibility with the processing unit.

Hardware-related tasks generally progressed as planned. Major updates include replacing the initial servo-based rotation mechanism with a more robust stepper motor system for azimuth control, and a high-torque DC motor for elevation. These changes improved mechanical reliability and range of motion. The motor driver was also upgraded to a more capable unit to prevent thermal issues and enable microstepping. Power capacity was increased with a larger Li-Po battery to ensure stable performance during extended operation.

In parallel, the team developed an in-lab signal emulation system that allows controlled testing of direction-finding algorithms without needing actual RF transmissions. This setup, along with a desktop interface for real-time monitoring and control, contributed to smoother debugging and system evaluation.

Overall, even though a few technical areas require more attention than initially expected, the project remains on track. The CDRR process helped clarify the architecture and finalize key design decisions. With core modules implemented and integration underway, the team is confident in meeting the final project timeline.

Discussions

Several safety considerations have been identified and addressed throughout the development of the RFATS system. Firstly, the system emits RF signals at 2 GHz using low-power SDR-based transmissions, which comply with regulatory exposure limits for non-ionizing radiation; however, direct prolonged proximity to transmitting antennas is avoided during operation. Secondly, the mechanical structure includes a fast-moving azimuthal motor system with speeds exceeding 150°/s with extending antennas; to prevent injury, physical access to moving parts is restricted during active tracking, and the design includes mechanical enclosures to shield exposed gears. Electrical hazards are also considered—especially given the use of a 3-cell Li-Po battery. Over-discharge protection circuits and voltage monitoring modules are implemented to prevent thermal runaway or short circuits. Furthermore, high-current lines are routed with thick, heat-resistant wiring to minimize the risk of overheating. Lastly, precautions during development included bench testing with current-limited supplies and software-defined fail-safes in both motor and power control modules to minimize the risk of system damage or user harm. In case of caution, the system can be shut down with a simple button from the GUI.

Our product, the RF-based Antenna Tracking System (RFATS), enables reliable and energy-efficient wireless communication by maintaining a directional line-of-sight (LOS) link without relying on GNSS data. This makes it particularly valuable in environments where GPS signals are unreliable or unavailable, such as remote rural areas, underground facilities, or conflict zones. A key societal impact is its potential to bridge communication gaps for mobile platforms like UAVs or emergency vehicles operating in these environments. Moreover, the underlying submodules—such as the direction-of-arrival estimation algorithms, signal synchronization strategies, and modular mechanical control systems can be repurposed for various industrial, scientific, or defense applications. By offering a compact, autonomous, and interference-resilient tracking capability, the system contributes to advancing critical infrastructure, disaster response, and secure field communications in both civilian and military sectors.

Lastly, while the RFATS system is designed to be compact and energy-efficient, potential environmental impacts have been considered, particularly in scenarios of widespread deployment. The system uses a 2 GHz frequency band, which does not interfere with wildlife-critical frequency bands or licensed spectrum if operated within regulated limits. However, in large-scale deployments, care must be taken to avoid frequency congestion in unlicensed bands. From a hardware perspective, the primary concern is the use of Li-Po batteries, which contain hazardous chemicals and require proper recycling to prevent soil and water contamination. To mitigate this, our design includes battery health monitoring features to extend operational lifespan and reduce electronic waste. The mechanical components are primarily composed of recyclable materials such as aluminum and 3D-printed PLA, allowing for environmentally conscious disposal. Additionally, the system's power-efficient design minimizes overall energy consumption, making it suitable for solar-powered or low-carbon

deployments in field operations. With responsible deployment and end-of-life recycling, the environmental footprint of RFATS remains minimal.

Conclusion

The RF-based Antenna Tracking System (RFATS) presented in this Critical Design Review has evolved into a functionally mature and structurally integrated platform capable of addressing real-time tracking challenges in GPS-denied and interference-heavy environments. Through a combination of directional RF signal reception, advanced signal processing, and precise mechanical actuation, the system offers a self-contained solution for maintaining communication lock with mobile RF sources.

The final design integrates multiple subsystems—antenna arrays, signal processing modules, motor control units, and a centralized power supply—into a compact and modular architecture. Each component was selected and developed based on specific performance criteria, such as angular accuracy under 5 degrees RMS, tracking speeds exceeding 15 degrees per second, and rapid reacquisition capabilities within 3 seconds of signal loss. These metrics were validated through both analytical modeling and early-stage testing, demonstrating the system's responsiveness and adaptability under constrained conditions.

One of the most critical advancements since the conceptual phase has been the full transition of signal processing algorithms from MATLAB to C++, enabling real-time execution on a Raspberry Pi 5 and allowing for seamless integration with hardware-level control logic. This transition, along with the redesign of the mechanical tracking system, most notably the replacement of servo motors with a high-torque stepper and geared DC motor configuration—has improved system reliability and expanded its operational limits. Despite these upgrades, certain areas such as downward elevation stability still present challenges, which are being actively addressed through updated torque specifications and control strategies.

The subsystem compatibility, interface coherence, and synchronization mechanisms developed throughout this phase have laid the foundation for a robust and extensible tracking platform. All functional modules communicate through well-defined protocols, and power distribution has been optimized to support long-duration operation with appropriate protection and monitoring.

In conclusion, RFATS now stands as a cohesive, real-world-capable system that meets its initial design goals and offers flexibility for future enhancement. The report comprehensively documents the development journey—from requirement formulation and architectural design to subsystem implementation and evaluation—and serves as both a technical reference and a roadmap for the final integration and testing stages that will follow in the remaining project timeline.

References

- [1]: AD9361 User Manual <https://www.analog.com/en/products/ad9361.html>
- [2]: <https://wiki.analog.com/resources/tools-software/linux-software/libiio>
- [3]: <https://datasheets.raspberrypi.com/rpi5/raspberry-pi-5-product-brief.pdf>
- [4]: <https://www.analog.com/media/en/technical-documentation/data-sheets/HMC7992.pdf>
- [5]: <https://pages.pbclinear.com/rs/909-BFY-775/images/Data-Sheet-Stepper-Motor-Support.pdf>
- [6]: <https://www.robotpark.com/12V-10Rpm-L-Geared-DC-Motor-KWL-FP>

Appendix

A1.1 Scattering Parameters of 2.4GHz Yagi-Uda Antenna



A2. Test Results

Table A2.1: Search Test

Parameter Value	Actual Performance	Expected Performance	Error
30°	4.03 s	Reach $\pm 5^\circ$ range under 3 seconds	1.13 s
60°	3.79 s	Reach $\pm 5^\circ$ range under 3 seconds	0.98 s
90°	3.83 s	Reach $\pm 5^\circ$ range under 3 seconds	0.73 s
120°	3.41 s	Reach $\pm 5^\circ$ range under 3 seconds	0.58 s
150°	3.36 s	Reach $\pm 5^\circ$ range under 3 seconds	0.36 s
180°	3.28 s	Reach $\pm 5^\circ$ range under 3 seconds	0.28 s
210°	2.96 s	Reach $\pm 5^\circ$ range under 3 seconds	0 s
240°	2.68 s	Reach $\pm 5^\circ$ range under 3 seconds	0 s
270°	2.39 s	Reach $\pm 5^\circ$ range under 3 seconds	0 s
300°	2.54 s	Reach $\pm 5^\circ$ range under 3 seconds	0 s
330°	2.46 s	Reach $\pm 5^\circ$ range under 3 seconds	0 s
360°	2.52 s	Reach $\pm 5^\circ$ range under 3 seconds	0 s

Table A2.1: Tracking Performance Test

Parameter Value	Actual Performance	Expected Performance	Error
45°	1.7 s	Arrive desired degree less than 3s	0 s
90°	2.9 s	Arrive desired degree less than 6s	0 s
135°	4.3 s	Arrive desired degree less than 9s	0 s
180°	7.0 s	Arrive desired degree less than 12s	0 s
225°	8.7 s	Arrive desired degree less than 15s	0 s
270°	9.4 s	Arrive desired degree less than 18s	0 s
315°	10.8 s	Arrive desired degree less than 21s	0 s
360°	12.6 s	Arrive desired degree less than 24s	0 s

Table A2.3: Azimuth Tracking Test

Parameter Value	Actual Performance	Expected Performance	Error
1m	2.91°	Less than ±5° range tracking error	0°
1m	2.16°	Less than ±5° range tracking error	0°
1m	2.04°	Less than ±5° range tracking error	0°
1m	3.23°	Less than ±5° range tracking error	0°
1m	1.97°	Less than ±5° range tracking error	0°
3m	2.01°	Less than ±5° range tracking error	0°
3m	1.71°	Less than ±5° range tracking error	0°
3m	1.66°	Less than ±5° range tracking error	0°
3m	1.85°	Less than ±5° range tracking error	0°
3m	1.22°	Less than ±5° range tracking error	0°
5m	2.23°	Less than ±5° range tracking error	0°
5m	1.88°	Less than ±5° range tracking error	0°
5m	1.84°	Less than ±5° range tracking error	0°
5m	1.71°	Less than ±5° range tracking error	0°
5m	2.12°	Less than ±5° range tracking error	0°

Table A2.4: Elevation Tracking Test

Parameter Value	Actual Performance	Expected Performance	Error
1m	4.06°	Less than ±5° range tracking error	0°
1m	3.98°	Less than ±5° range tracking error	0°
1m	3.44°	Less than ±5° range tracking error	0°
1m	5.12°	Less than ±5° range tracking error	0.12°
1m	4.40°	Less than ±5° range tracking error	0°
3m	5.08°	Less than ±5° range tracking error	0.08°

3m	4.66°	Less than ±5° range tracking error	0°
3m	4.27°	Less than ±5° range tracking error	0°
3m	4.12°	Less than ±5° range tracking error	0°
3m	5.23°	Less than ±5° range tracking error	0.23°
5m	6.11°	Less than ±5° range tracking error	1.11°
5m	5.48°	Less than ±5° range tracking error	0.48°
5m	4.96°	Less than ±5° range tracking error	0°
5m	5.67°	Less than ±5° range tracking error	0.67°
5m	5.02°	Less than ±5° range tracking error	0.02°

A3. User Manual